The Sixth International Workshop on Micro and Nanotechnology for
Power Generation and Energy Conversion Applications, Nov. 29 - Dec. 1, 2006, Berkeley, U.S.A.

CHARACTERIZING NON-PREMIXED SUB-MILLIMETER COMBUSTION

Shaurya Prakash[1], Adrian D. Armijo[1], Richard I. Masel[2], Mark A. Shannon[1*]

[1] University of Illinois at Urbana-Champaign, Department of Mechanical Science and Engineering
1206 W. Green Street, Urbana, IL 61801 U.S.A.
[2] University of Illinois at Urbana-Champaign, Department of Chemical and Biomolecular Engineering
600 S. Mathews, Urbana, IL 61801 U.S.A.
[*] Corresponding Author: mshannon@uiuc.edu

Abstract

This paper presents one of the first reports on flame dynamics and structure observed in non-premixed methane-oxygen combustion at the microscale for power generation. The flame dynamics and structure are evaluated from ignition to the formation of stable flame cells within alumina (Al_2O_3) combustors with a combustor volume of ~ 130 mm^3 with the smallest dimension of 0.75 mm. Flame behavior is characterized using high-speed imaging, still-frame imaging, chemiluminescence measurements, recording of acoustic emissions from the combustor, and measurement of combustor wall temperature profiles. Imaging and acoustic data provide insight into the flame dynamics and the flame stabilization process. Chemiluminescence data is collected for visible, OH^*, and CH^*. These results suggest that the observed flame behavior is characteristic of hydrodynamic instabilities being eventually stabilized by the thermal-fluid interactions present in reacting flows.

Keywords: Alumina (Al_2O_3), Microheater, Methane, Non-premixed combustion, Flame structure

1 - INTRODUCTION

Many different approaches are being used to address the issues in developing systems for micropower generation (MPG). For instance microengines [1-3], microburners [4-7], micro fuel cells [8, 9], thermal vapor cycles [10], thermoelectric [11], and thermophotovoltaic systems [12] are being developed to meet the increasing demands of MPG and microscale heat sources. Despite a broad range of research and several advancements in the field of micro-and meso-scale combustion for MPG many open questions remain for constructing systems that provide predictable and controllable heat output with uniform wall temperatures that can be operated for extended time periods to meet the promise of combustion-based portable and personal power sources. Toward the continued effort in developing appropriate heat sources for MPG, a sub-millimeter or microscale combustor has been developed to act as a heat source for the multitude of intended applications [13]. However, microscale combustion systems are characterized by high surface area to volume ratio leading to thermal quenching due to excessive heat loss to the combustor walls and chemical quenching due to destruction of key radicals at the combustor walls. Thus, initiating and sustaining homogeneous combustion can be a challenge. Therefore, understanding the dynamics of the combustion process is helpful to control the heat output of microcombustors. In this paper, flame dynamics and structure observed in non-premixed methane-oxygen combustion at the microscale in alumina combustors are reported. The flame dynamics and structure are evaluated from ignition to the formation of stable flame cells within alumina (Al_2O_3) combustors with a combustor volume of ~ 130 mm^3 and with the smallest dimension of 0.75 mm. Flame behavior is characterized using high-speed imaging, still-frame imaging, chemiluminescence measurements, recording of acoustic emissions from the combustor, and measurement of combustor wall temperature profiles.

2 - EXPERIMENTAL DESCRIPTION

Material preparation to minimize radical quenching and procedure for burner fabrication have been reported previously [4-7, 14, 15]. Briefly, the Al_2O_3 non-premixed sub-millimeter or microcombustors are machined from 1 mm thick α-phase polycrystalline alumina sheets (96% purity from McMaster-Carr). The sheets are machined into two identical Y-shaped pieces, with each leg having a width of 10 ± 0.5 mm and length of 35 ± 0.5 mm. A 5 ± 0.5 mm wide by 0.375 mm deep channel is machined into the center of the pieces, so when assembled the total depth is 0.75 ± 0.1 mm. In one of the alumina pieces, a slot is machined to fit a 36 mm x 7 mm C-plane sapphire piece to provide a window for imaging of the flame dynamics. The gases come into the reaction channels right angles with respect to each other (Fig. 1A). The machined alumina pieces are cleaned using a standard degrease procedure with acetone and isopropyl alcohol followed by the standard RCA-2 clean (DI $H_2O/HCl/H_2O_2$ in 4:1:1 ratio by volume) at 60°C to remove metallic contaminants that may be on the alumina surfaces. Next, a two-step anneal process is carried out [6, 15]. This two-step anneal process is thought to reduce surface defects and minimizes oxygen vacancies that can exist in alumina

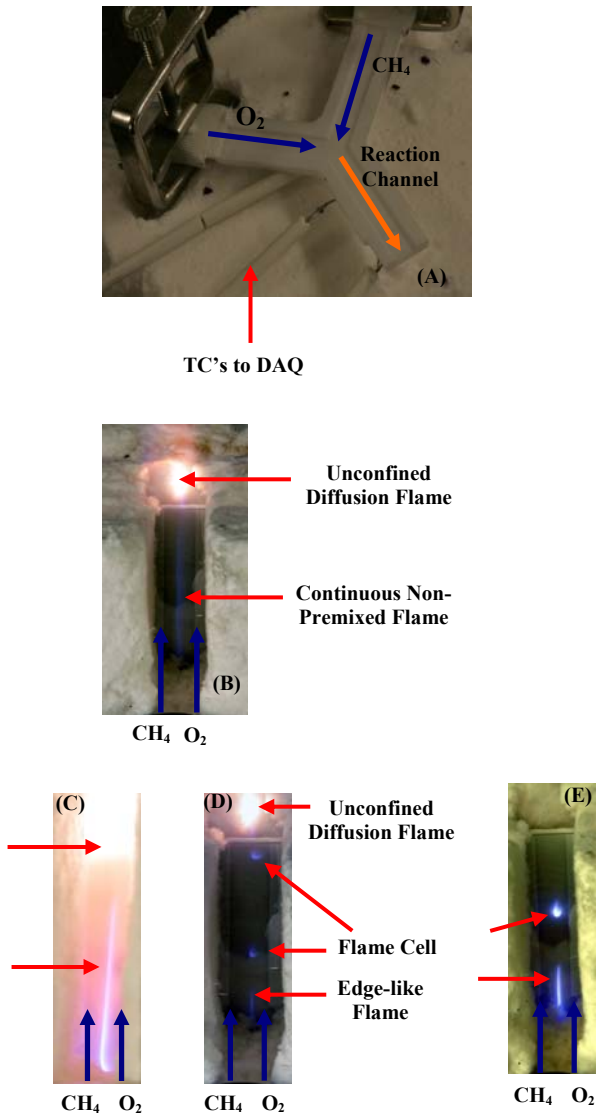

Figure 1: **(A)** An image of the combustor with a sapphire window on the top side for flame imaging. The thermocouples (TCs) used to measure combustor wall temperatures are shown in the figure. The channel dimensions are 35 mm x 5 mm x 0.75 mm. **(B)** Still-frame image captured immediately after ignition. **(C)** Still-frame image at flow rates of 200 sccm O_2 and 100 sccm CH_4 captured after combustor operation for an extended time, the red glow from the hot combustor walls (> 600°C) is seen. **(D)** The flame cell comprising of an edge-like flame near the gas inlet and individual flame cells. **(E)** Operation of the combustor in steady-state with a single flame cell. Equal flow rate of fuel and oxidiser (total flow rate 300 sccm) in all images, except image (C).

[16]. The polycrystalline alumina and sapphire pieces are annealed in an argon atmosphere at 1550°C for one hour followed by a second anneal at 1100°C in an oxygen atmosphere for 10 hours. All the machined, cleaned, and annealed components are manually aligned and bonded with an Aremco 569 high-temperature ceramic adhesive (Aremco Inc., Valley Cottage, NY) to yield the final device. Type R thermocouples (TCs) obtained from Omega Engineering Inc. (Stamford, CT) are located along the outside wall of the alumina combustor and connected to a data acquisition system to obtain external wall temperature profiles during combustor operation as a function of time. High purity methane (CH_4) and oxygen (O_2) gases are controlled by M100B MKS mass flow controllers, and flow through attached hoses. The entire assembly is then packed in between two approximately 2.5 cm thick insulation layers of fibrous alumina. The exhaust and unburnt gases flow freely into the ambient air (Fig. 1).

The flame dynamics were imaged via still-frame and high-speed imaging. The still-frames are captured by a Canon EOS Mark II digital camera with an attached infrared filter, and the high-speed images are acquired by using a Vision Research Inc. camera (model no. Phantom v7.1). The OH* and CH* chemiluminescence was captured using an Andor Technology iCCD camera (South Windsor, CT, Model No. DM712-18F-03). The camera settings for all intensity profiles used a 0.1 s exposure time with a gate width of 100 μm. The OH* chemiluminescence was isolated by using a narrow bandpass filter (Andover Corporation, Salem, NH) centered at 307 nm with a 10 nm bandwidth and a peak transmittance of 19%. The CH* chemiluminescence was isolated using a narrow bandpass interference filter (Edmund Optics, Barrington, NJ) centered at 430 nm with a 10 nm full-width half-maximum. The emitted sound was recorded using a Knowles Acoustic (Itasca, IL) microphone (model no. FG-3329) at a sampling rate of 20 kHz to give a 2.5 times over Nyquist sampled maximum frequency of 4000 Hz reported here. The microphone was connected to a pre-amplifier and a Hewlett-Packard (model no. 54645D) oscilloscope to monitor the acoustic signal. In addition, the measured signal was recorded using a computer-controlled data acquisition system.

3 - RESULTS AND DISCUSSION

One of the ways to better understand the microcombustion process is to observe and characterize the entire sequence of events from ignition to the formation of steady-state, stable flame structures. Three different imaging techniques, acoustic measurements, and combustor wall measurements were carried out to characterize the observed flame dynamics and structures. Imaging and acoustic data provide insight into the flame dynamics and the flame stabilization process. As the observed steady-state flame structure (Fig. 1D and 1E) is discontinuous and comprising of distinct reaction (flame) and mixing zones temperature profiles can provide valuable clues with respect to the effect of heat loss on flame stabilization. Figure 1 shows the still-frame images of the combustor in various stages of operation. The combustors can be operated in a variety of different modes depending on the inlet flow rates, combustor wall temperature, and surrounding boundary

conditions. Figure 1E shows the steady-state operation of the combustor with a single flame cell. The number and spacing of flame cells can also be controlled by varying the inlet flow conditions.

Figure 2A shows the high-speed images captured at early times after ignition. Figure 2A shows that the continuous flame observed in Fig. 1B is actually a collection of rapidly traveling individual flames at a frequency of ~ 142 Hz. Figure 2B shows that the flame cells form and stabilize by an ignition/extinction event. This event progresses at a frequency of about 65 Hz. In addition, it is seen that the edge-like flame near the combustor inlet oscillates laterally at ~ 90 Hz.

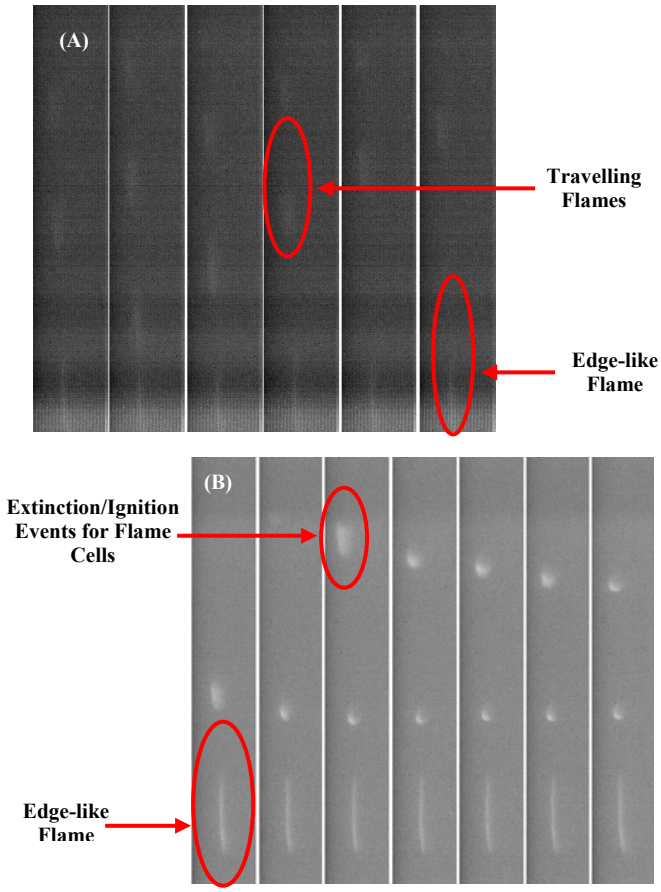

Figure 2: **(A)** High-speed image taken at 1000 frames per second at early times after ignition shows that in contrast to the continuous flame seen in Fig. 1B the flame structure consists of rapidly moving individual flames. **(B)** High-speed images taken at 500 frames per second showing the stabilization of the top flame cell. The bottom flame cell stabilizes first by the same ignition/extinction phenomena at a frequency of about 65 Hz. Equal flow rate of fuel and oxidiser (total flow rate 300 sccm) in all images.

Figure 3A shows an example of the steady-state temperature profile of the combustor wall. The top, middle, and bottom TCs refer to thermocouples attached to the outside of the combustor wall starting near the exhaust and moving down toward the inlet. The TCs are placed at 0.5, 1.5, and 2 cm from the combustor exhaust. Chemiluminescence provides estimates of the inter-diffusion of the oxidizer (O_2) and fuel (CH_4) during the combustion process (Fig. 3B). It is seen in Fig. 3B that the flame cells have a hook-like structure with the curved end always pointing to the oxygen side. Figures 3C and 3D show representative data of the acoustic emission from the combustor during the transient phase before flame stabilization showing two main kinds of frequencies; first is the structural interaction of the combustor with the reacting flows and second the frequencies displayed by the flame dynamics. Strouhal number analysis [6] of the flame dynamics indicates that the observed flame behavior is characteristic of hydrodynamic instabilities being eventually stabilized by the thermal-fluid interactions present in reacting flows.

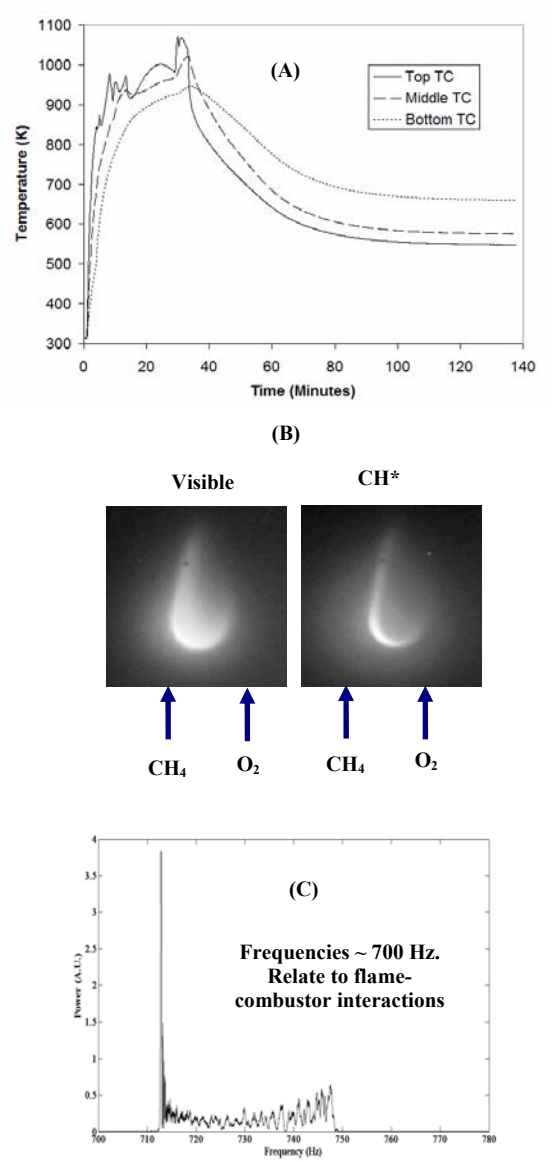

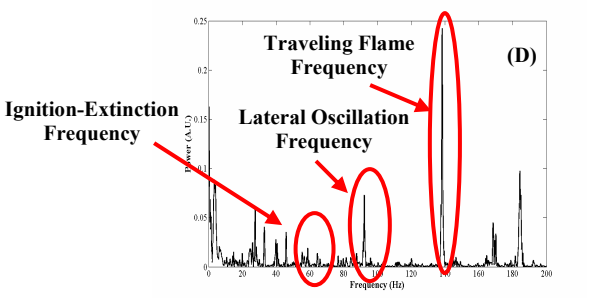

Figure 3: **(A)** Steady-state combustor wall temperature profile. **(B)** High-resolution visible and CH* chemiluminescence images show flame cells have hook-like structure. **(C)** High frequencies (not seen in imaging relate to combustor structure and flame interactions. **(D)** Low frequency components related to flame dynamics.

4 - CONCLUSIONS

Flame dynamics and resulting steady-state flame structures have been characterized. Flame imaging shows that the flame structure consists of traveling and oscillating flame structures due to hydrodynamic instabilities after ignition. As the combustion process continues and the walls and gases heat up, distinct, stable flame cells form. These flame cells have a hook-like structure with the curved end always pointing to the oxygen or lean side. It is hoped that these observations of flame dynamics and structures will lead to a better understanding of the combustion processes at these length scales and provide for improved high-temperature microcombustors for power generation.

ACKNOWLEDGMENTS

This work was supported by the Department of Defense Multidisciplinary University Research Initiative (MURI) program administered by the Army Research Office under grant DAAD19-01-1-0582. The authors thank Jeahyong Han, Jessica Mullen, Robert Covderdill, Prof. C.F. Lee, Prof. D.C. Kyritsis, Kowtilya Bijjula, Craig Miesse, Chaitanya Gupta, and Dillon Yoshitomi for assistance during various phases of this work.

REFERENCES

[1] Aichlmayr, H.T., *Design considerations, modeling, and analysis of micro-homogeneous charge compression ignition combustion free-piston engines*. 2002, University of Minnesota.

[2] Knobloch, A.J., M. Wasilik, C. Fernandez-Pello, and A.P. Pisano. Micro, internal-combustion engine fabrication with 900 μm deep features via DRIE. in *Proceedings of the ASME International Congress and Exposition.* 2003. Washington, D.C., USA. .

[3] Mehra, A., X. Zhang, A.A. Ayon, I.A. Waitz, M.A. Schmidt, and C.M. Spadaccini, 2000, A six-wafer combustion system for a silicon micro-gas turbine engine. *Journal of Microelectromechanical Systems*. **9** 517-527.

[4] Miesse, C.M., R.I. Masel, C.D. Jensen, M.A. Shannon, and M. Short, 2004, Submillimeter-scale combustion. *AIChE Journal*. **50** 3206-3214.

[5] Prakash, S., A.D. Armijo, R.I. Masel, and M.A. Shannon. Unsteady flames in microcombustion. in *ASME International Mechanical Engineering Congress and Exposition*. 2006. Chicago, IL.

[6] Prakash, S., A.D. Armijo, R.I. Masel, and M.A. Shannon, In Press, Flame dynamics in sub-millimeter combustors. *International Journal of Alternative Propulsion*.

[7] Prakash, S., C.M. Miesse, R.I. Masel, and M.A. Shannon, 2005, Flame structure variations in sub-millimeter combustors due to heat transfer through combustor walls. *Proceedings of the Fourth Joint Meeting of the U.S. Sections of the Combustion Institute*.

[8] Chu, K.L., S. Gold, V. Subramanian, C. Lu, M.A. Shannon, and R.I. Masel, 2006, A nanoporous silicon membrane electrode assembly for on-chip micro fuel cell applications. *Journal of Microelectromechanical Systems*. **15** 671-677.

[9] Ha, S., Z. Dunbar, and R.I. Masel, 2006, Characterization of a high performing passive direct formic acid fuel cell. *Journal of Power Sources*. **158** 129-136.

[10] Lee, C., M. Liamini, and L.G. Fréchette. Design, fabrication, and characterization of a microturbopump for a Rankine cycle micropower generator. in *Solid-State Sensors and Actuators Workshop*. 2006. Hilton Head Island, SC. . 276-279

[11] Vican, J., B.F. Gajdeczko, F.L. Dryer, D.L. Milius, I.A. Aksay, and R.A. Yetter, 2002, Development of a microreactor as a thermal source for microelectromechanical systems power generation. *Proceedings of the Combustion Institute*. **29** 909-916.

[12] Yang, W.M., S.K. Chou, C. Shu, H. Xue, Z.W. Li, D.T. Li, and J.F. Pan, 2003, Microscale combustion research for application to micro thermophotovoltaic systems. *Energy Conversion and Management*. **44** 2625-2634.

[13] Dunn-Rankin, D., E.M. Leal, and D.C. Walther, 2005, Personal power systems. *Progress in Energy and Combustion Science*. **31** 422-465.

[14] Miesse, C.M., *Development of microcombustors and characterization of confined sub-millimeter laminar diffusion flames*, in *Department of Chemical and Biomolecular Engineering*. 2005, University of Illinois: Urbana.

[15] Prakash, S., N.G. Glumac, N. Shankar, and M.A. Shannon, 2005, OH concentration profiles over alumina, quartz, and platinum surfaces using laser-induced fluorescence spectroscopy in low-pressure hydrogen/oxygen flames. *Combustion Science and Technology*. **177** 793-817.

[16] Henrich, V.E. and P.A. Cox, *The surface science of metal oxides*. 1994, Cambridge: Cambridge University Press.